

# Thermal model of bidirectional DC/DC converter

Evgeni Malev

*The purpose of this article is to create and analyze a mathematical model of Isolated full-bridge bidirectional DC/DC converter for electric vehicle application. The article considers and analyzes mathematical models of the proposed topology converter through the software products Comsol and Matlab. The models describe the thermal processes that take place between the main components of the converter and the power switch heatsink.*

**Keywords:** DC-DC converter, thermal model, heatsink, Isolated full-bridge bidirectional DC-DC converter, Comsol.

*Топлинен модел на двупосочен DC/DC преобразувател (Евгени Малев). Целта на тази статия е анализирането и създаването на математически модели на Мостов изолиран двупосочен импулсен преобразувател за постоянно напрежение, намиращ приложение в електрически автомобили. Статията разглежда и анализира математически модели на предложената топология на преобразувател чрез софтуерните продукти Comsol и Matlab. Моделите описват термичните процеси, които протичат между основните компоненти на преобразувателя и радиатора на превключвателя на захранването.*

## 1. Introduction

DC-DC converters are widely used in automation and industry, renewable energy sources, electric transport, power supplies and others. They are operating in different modes and have losses from conductivity, switching and heat. The uncontrolled temperature rise can seriously damage or lead to deformation or destruction of part of the converter or the entire device.

The input power of a DC - DC converter is not always equal to the output, due to the dissipation of part of the power in the form of heat. The junction temperature and total power absorbed from the transistor can be expressed by [1]:

$$(1) \quad \Delta T = R_{th} \cdot P_{diss} - T_a$$

$$(2) \quad P_{diss} = I_{ds} \times V_{ds}$$

where  $\Delta T$  is the junction temperature,  $P_{diss}$  is the instantaneous total power absorbed in the transistor, and  $T_a$  - the ambient temperature,  $V_{ds}$  and  $I_{ds}$  are voltage and current Drain – Source of the transistor.

A thermal model of an electronic converter is created in order to analyze the behavior of temperatures and heat fluxes in the different parts of

the circuit. To create a thermal model of a converter, it is necessary to use three main components, which are describing the thermal processes: 1) thermal radiation - electromagnetic radiation generated by the thermal motion of particles in matter [2]. 2) Heat conduction - the capability of solid matter to transfer heat (in power electronics, most often semiconductors, metal, dielectric or other material). 3) Convection - heat transfer from one point to another in a medium - fluid or air. The heat conduction can be expressed by the equation:

$$(3) \quad \frac{\partial}{\partial x} \left( k \frac{\partial T}{\partial x} \right) + \frac{\partial}{\partial y} \left( k \frac{\partial T}{\partial y} \right) + \frac{\partial}{\partial z} \left( k \frac{\partial T}{\partial z} \right) + q_v = \rho c_p \frac{\partial T}{\partial t}$$

where  $k$  – is material conductivity [ $\text{W} \cdot \text{m}^{-1} \cdot \text{K}^{-1}$ ],  $c$  - specific heat capacity [ $\text{J} \cdot \text{kg}^{-1} \cdot \text{K}^{-1}$ ],  $\rho$  - material density [ $\text{kg}/\text{m}^3$ ],  $q_v$  is the rate at which energy is generated per unit volume of the medium [ $\text{W} \cdot \text{m}^{-3}$ ] [2].

The equivalent circuit of a thermal model can be created by R - C branches, voltage and current sources, which express the thermal behavior of the electronic components of the converter.

Figure 2 presents a thermal model of a DC-DC converter derived from Ohm's Law [3].

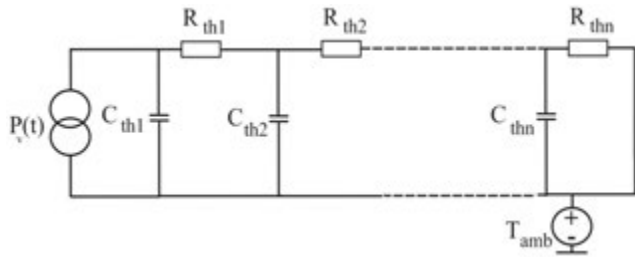


Fig. 1. Equivalent circuit of the thermal process.

The components of the equivalent circuit are  $P_v(t)$  heat flow to the circuit,  $R_{th1}$ ,  $R_{th2}$ ,  $R_{thn}$  – series thermal resistance  $C_{th1}$ ,  $C_{th2}$ ,  $C_{thn}$  - series thermal capacitance of each branch of the circuit,  $T_{amb}$  – ambient temperature of the circuit. The equivalent scheme gives us an idea of how the heat exchange between the individual components in the converter develops. On Fig.1 heat transfer is specific depending on the materials from which the components are made, their size and location, construction and type of cooling system. The analysis of thermal processes is performed by converting the thermal components into electrical ones [4].

Table 1

Comparison of the quantities electrical and thermal model of an electronic circuit

Electrical model	Thermal model
Electrical current I [A]	Thermal power $P_D$ [W]
Voltage U [V]	Temperature °C
Resistance R [ $\Omega$ ]	Thermal resistance $R_{\theta_{xy}}$ [°C/W]
Capacity C [F]	Thermal capacitance $R_{\theta_{xy}}$ [J/°C]

In the model electrical current, potential difference or voltage, resistance and capacity are equivalent to thermal power, temperature, thermal resistance and thermal capacity. Thermal processes develop similarly to electrical processes in individual branches and we can find a relationship between them by Ohm's law and other dependences in electromagnetism [5].

## 2. Modelling an isolated full-bridge bidirectional DC-DC converter in Matlab

The isolated bidirectional full-bridge dc-dc

converter is a topology with high conversion ratio and high output power. It finds application in power supplies, battery chargers, electric vehicles, power inverters and others. It consists mainly of two parts – high and low side, galvanically separated by a high frequency transformer [6]. A filter capacitor / capacitors are placed at the input and output of the converter. Depending on the application and for greater efficiency, an additional scheme for soft start can be placed on the high side [7]. This isolated full bridge bidirectional DC-DC converters are most complex and expensive in comparison with other topologies, but is characterized by the highest efficiency (up to 70-80%) and low voltage stress levels during commutation. The scheme of the converter is presented in Fig.2. The power switches are controlled by PWM generated by a microcontroller and fed to each switch via a driver [8], [9], [10]. On Figure 4 is shown the modeled converter in the computing platform Matlab. It is composed of bridge capacitors on the input – C1 and C2; high side power switches – Q1, Q2, Q3; low side power switches - Q5, Q6, Q7 and Q8; isolated high frequency transformer – T; filter capacitor – C3.

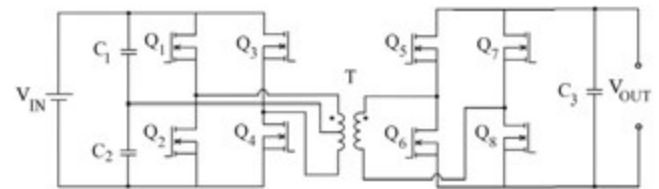


Fig. 2. Circuit of bidirectional DC-DC converter.

In the MATLAB programming environment, a mathematical model of an isolated full-bridge bidirectional DC-DC converter is created to study its input-output parameters, currents and voltages on each switch and the relationship with the heatsink.

Figure 3 shows a Isolated full-bridge bidirectional DC-DC converter with input capacitor filter for reduction current ripple, modeled in Matlab.

The control of the circuit is realized by blocks from the library Fundamentals: Pulse generators, Repeating sequence, Transport delay and relation operator. They create a control unit, which generates PWM to each key depending on the operating modes.

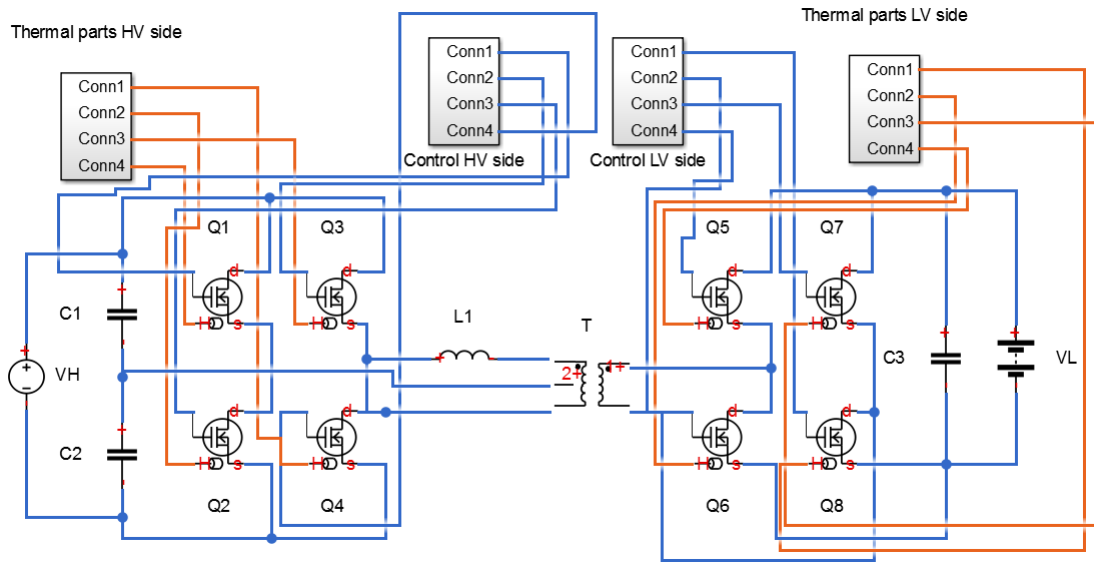


Fig.3. Model of isolated full-bridge bidirectional DC-DC converter in Matlab.

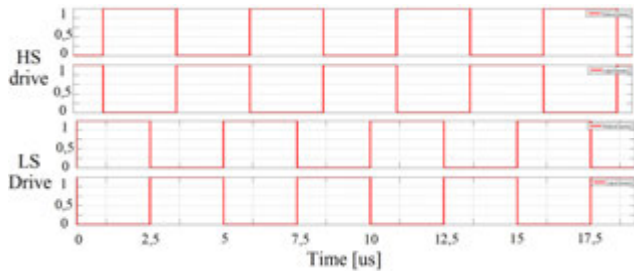


Fig.4. Waveforms of the control unit of the isolated full-bridge bidirectional DC-DC converter in Matlab

The input-output parameters are defined in Table 2. On the high side, a voltage source is used and on the low side a battery block were used. In step-up mode the converter charge the battery and the energy flows from the DC bus to the battery. In step-down mode, the energy flows from the battery to the bus.

Table 2

Main parameters of the converter

Parameter	Value
High side voltage:	400 V
Low side voltage	48 V
Capacitor 1,2	660 $\mu$ F
Capacitor 3	330 $\mu$ F
Inductor	228 $\mu$ H
Rated power	2 kW
Battery current	up to 60 A
Bus current	up to 5 A
Switching frequency $F_{sw}$	200 kHz

The junction temperature and the switching losses from the MOSFET are the major criteria to choose an

efficient power transistor. The main modelled Power MOSFET for the study is IXTK120N65X2. On Fig.5 a thermal circuit of a power transistor is shown [11], [12].

On the equivalent circuit  $R_{th CP}$  is the thermal chip-package resistance,  $R_{th PH}$  is the thermal package-heat sink resistance,  $R_{th HA}$  is the thermal heat sink-ambient air resistance [13].

The parameters in Table 3 are decisive when setting the parameters of the power switches in Simulink model. The currents and voltages of the MOSFETs in step-up (boost) and step-down (buck) mode can be seen in Fig.6 and Fig.7.

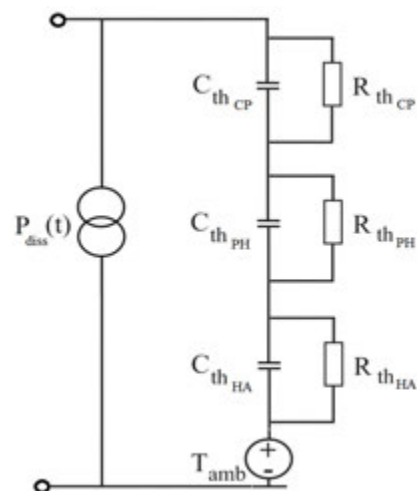


Fig.5. Thermal equivalent circuit of a power MOSFET transistor.

**Table 3**

Parameters of the power transistor used in the simulation models

Parameter	Value
Drain-to-Source Voltage $V_{DS}$	650 V
Drain-to-source On Resistance $R_{DS(ON)}$	2.5 m $\Omega$
Continuous Drain Current $I_D$	120 A
Power Dissipation	200 W
Gate Charge Gate to Drain $Q_{gd}$	14 nC

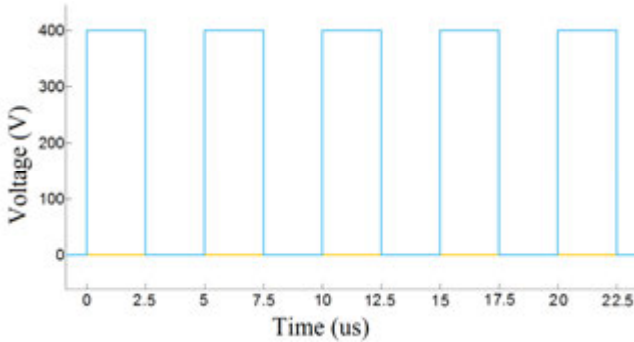


Fig. 6.  $V_{gs}$  of Q1 and voltage of the internal diode in step-up mode.

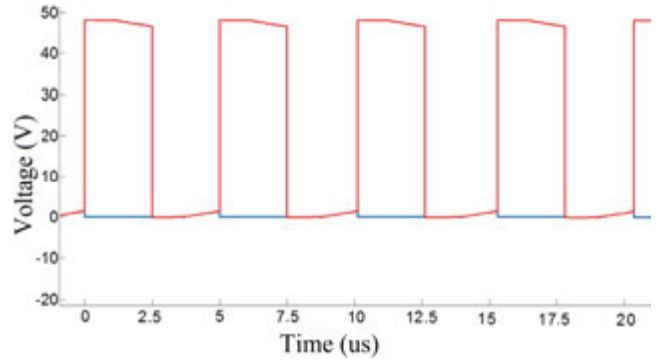


Fig. 7.  $V_{gs}$  of Q7 and voltage of the internal diode in Step-Down mode.

The dissipated energy from the MOSFET can be analyzed by a mathematical model, build with thermal components from the Simscape library.

The rise of the junction temperature from the MOSFET to the heatsink can be expressed with the blocks: conductive heat transfer for junction-case and junction-heatsink; conductive heat transfer for the heat dissipated from the heatsink in the air. In these blocks, constants related to the area, weight and energy density absorbed and emitted by each element are determined [14]. Figure.9 shows the change of

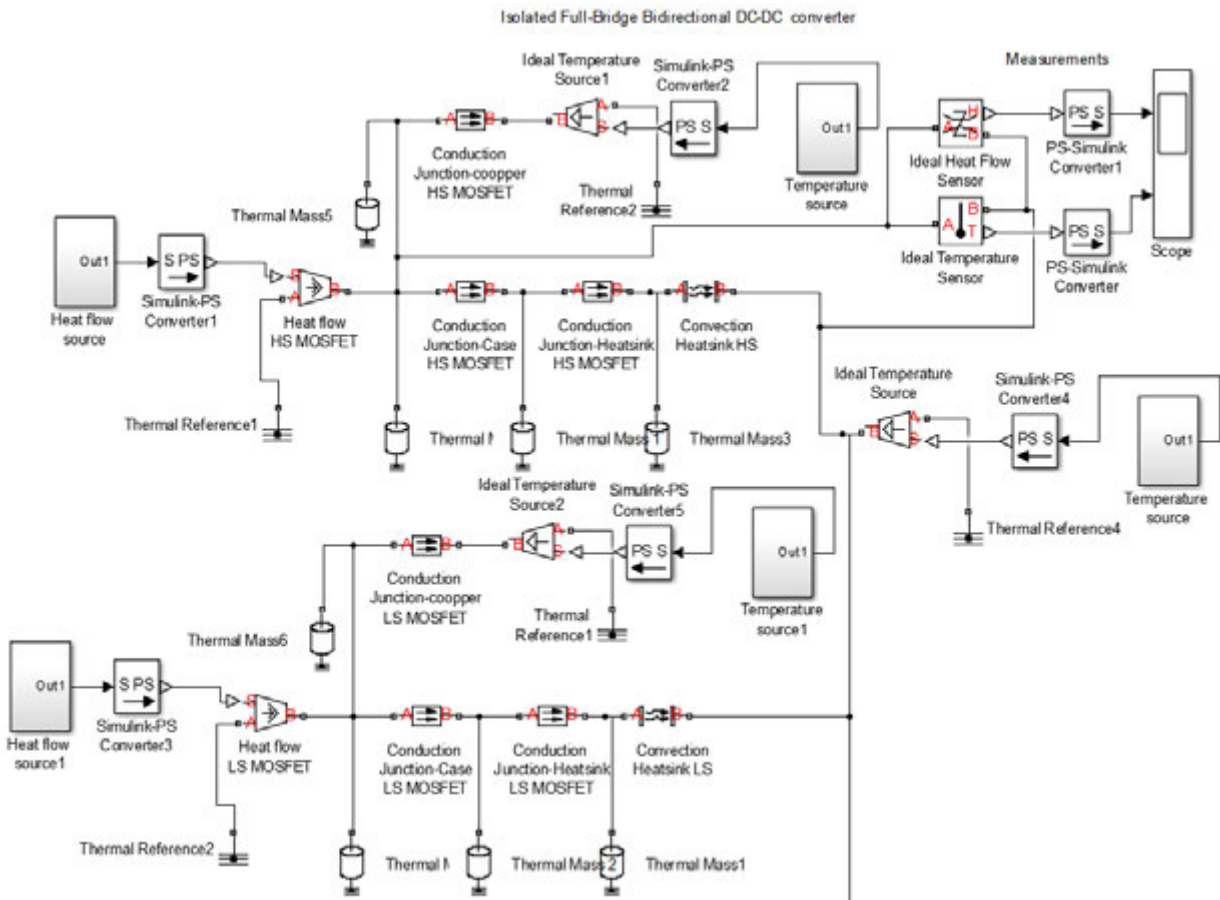


Fig. 8. Model of the heatsink in Matlab.

temperature in separate parts (points) of the thermal model of converter's transistor Q1 [15].

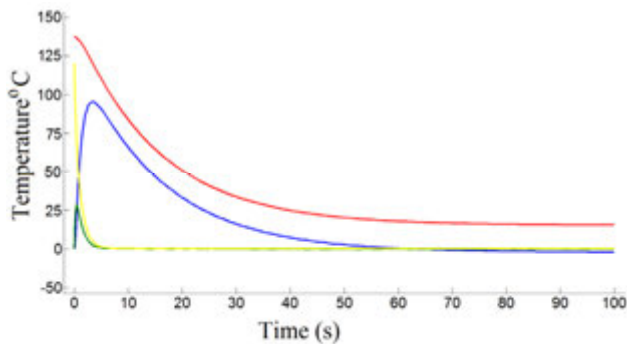


Fig. 9. Graph of temperature change on Q1 in step-up mode in junction – case (red), heatsink (blue), cooper track (green), convection heatsink (yellow).

Fig.10 shows the temperature of the power switch Q1 when the energy from the high side to the low side (blue) and from the low side to the high side (red).

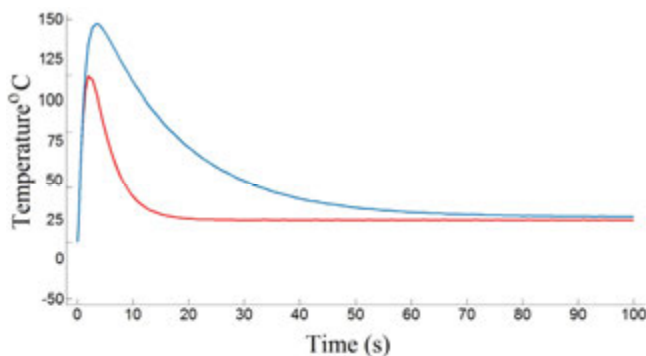


Fig. 10. Graph of temperature change on Q1 in step-up (blue) and step-down (red) mode.

The temperature graphs (Fig.9 and Fig.10) above show the change in temperature from step-up to sleeping mode. The ambient temperature of the model is simulated by a Simscape constant block - 25°C.

The heat flow of each one power switch in the two main operating modes is shown on Fig.11.

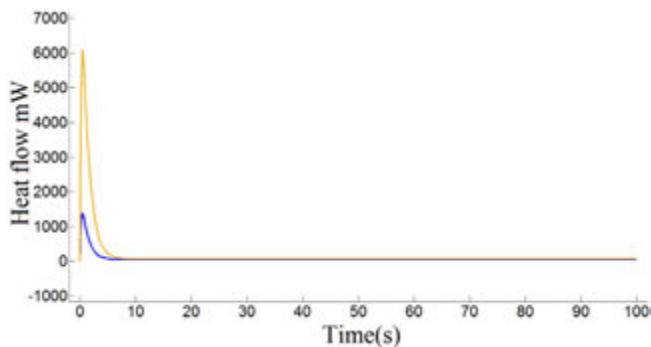


Fig. 11. Graph of thermal power change on Q1 in step-up (blue) and step-down (red) mode.

The three graphs shown give us information on the effective heat dissipation from the heatsink. It becomes clear that the heat dissipation is within the limits, as in the case of the physical element that is modeled [15].

### 3. Modelling an isolated full-bridge bidirectional DC-DC converter in Comsol

The Comsol programming environment allows the simulation of various physical objects. There are 20 libraries with semiconductor, magnetic, ferrite, dielectric and conductive materials. In addition, the program can simulate physical processes that develop in electronics. On Figure 12 is shown modeled Isolated Full-Bridge Bidirectional DC-DC converter with tetraeder mesh [16].

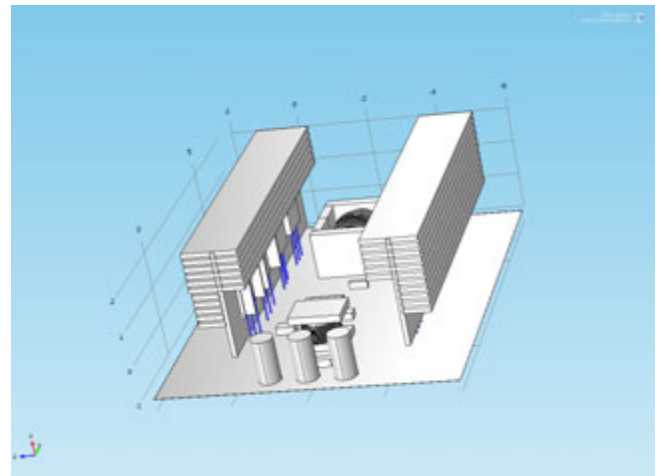


Fig.12. Model of a bidirectional DC-DC converter in Comsol.

Conductive, semiconductor, dielectric and magnetic materials have different thermal behavior. Table 4 shows the variables related to the thermal behavior of basic materials used in electronics.

The Thermal Expansion is expressed by the equation:

$$(4) \quad \frac{\Delta L}{L_0} = \alpha \Delta T$$

Where  $\Delta L$  is the change of the condition,  $L_0$  initial condition,  $\alpha$  - thermal quantity expansion,  $\Delta T$  - temperature change

The Wiedemann Franz's law is expressed by the equation:

$$(5) \quad \frac{k}{\sigma} = LT$$

where  $\sigma$  is electrical conductivity,  $k$  is thermal conductivity,  $L$  - Lorentz number and  $T$  - temperature [17].

**Table 4**

Thermal coefficients of some of the main materials used in electronics, where  $c_p$  is specific heat capacity ( $J.g^{-1}.K^{-1}$ ), thermal expansion -  $\alpha_L$  ( $m^\circ C$ ), Wiedemann Franz's law -  $L$  ( $W\Omega K^{-2}$ ), heat transfer coefficient -  $k$  ( $W/m^2$ )

	$c_p$	$k$	$\alpha_L$	$L$
Aluminum	900	60	23.6	2.2
Cooper	386	30	17	2.25
PTFE	1050	1500	150	
Polyethylene	1850	1830	150	
Iron	448	230	11.8	2.71
Silicon	556	1.3	2.6	

Heat transfer of solids and electric current physical processes have been added to study the behavior of the converter. The main parameters which relate the used materials to the physical parameters are expressed in Table 5.

**Table 5**

Electrical parameters of the used materials, where 1 is electrical conductivity ( $M^{-1}L^{-3}T^3A^2$ ), 2 is relative permeability (1) and 3 is relative permittivity (1)

Material	1	2	3
Iron	$1.04 \times 10^7$	5000	$1.2 \times 10^{-11}$
Aluminum	$3.5 \times 10^7$	1.00002	$2.2 \times 10^{-12}$
Cooper	$5.98 \times 10^7$	0.99	-
Silicon	0.0167	0.99	11.68
FR4	$0.001 \times 10^{-12}$	1.02	4.2
Ferrite	-	19.2	5.6

The Seebeck coefficient (or thermoelectric sensitivity) for the semiconductor and conducting materials can be calculated by the formula:

$$(6) \quad S = -\frac{\Delta V}{\Delta T}$$

where  $\Delta V$  - voltage's change and  $\Delta T$  - temperature's change. Analyzed at steady state where the current density is zero everywhere. For aluminum is  $3.5\mu V/K$ , for cooper -  $6.5\mu V/K$  and for silicon is  $440\mu V/K$ . Table 6 shows the parameters of the heatsink and MOSFET in Comsol:

**Table 6**

Dimensions of the components in Comsol model

Parameter	mm (inch)
MOSFET Width case / pin	3.5 (0.13) / 0.5 (0.019)
MOSFET Height	16 (0.62)
MOSFET Length	9.7 (0.38)
Heatsink Width	29.9 (1.18)
Heatsink Height	25.4 (1)
Heatsink Length	149 (5.9)
PCB Width	3 (0.118)
IC Driver Width	4.1 (0.0164)
Capacitor diameter	10 (0.39)

On Figure 13 is shown the temperature distribution of the main components of the investigated topology Bidirectional DC-DC converter in Comsol. The voltage on the HV bus of the converter is 400V. The voltage on the secondary side to charge the battery is 48V (60V maximum voltage). For air temperature were used 25°C. The secondary (HV side) RMS current through the transformer is estimated to be 7.5 A. 12.5A were the current that charges the battery. All this values were modeled in the Comsol physical processes - Heat transfer of solids and Electrical current.

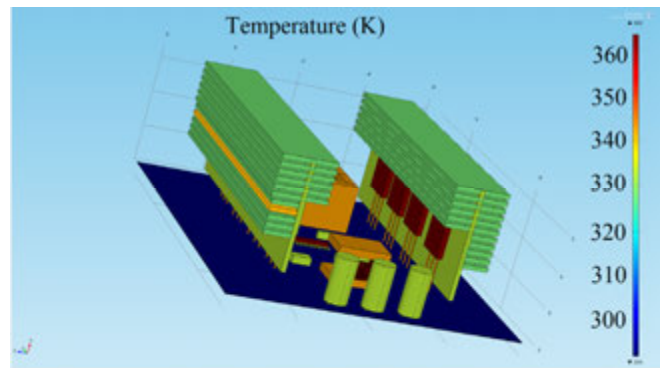


Fig. 13. Temperature distribution of isolated bidirectional Buck-Boost DC-DC converter in Comsol

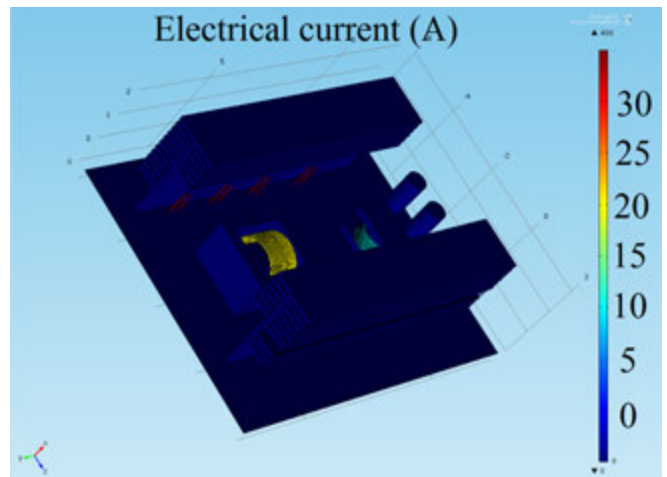


Fig. 14. Electrical current of the main components of the converter

#### 4. Power loss analysis of the converter

In order to calculate the thermal losses in a DC pulse converter, it is necessary to calculate the thermal losses in each active component. The basic equation of the thermal model is:

$$(7) \quad R_{th} = \frac{DT}{P_{diss}}$$

where  $R_{th}$  - thermal resistance,  $DT$  - temperature rise,  $P_{diss}$  - power dissipation.

Conduction losses on power MOSFET transistor are given on formula 8:

$$(8) \quad P_{avg} = P_{cm} + P_{bm} + P_{son} + P_{soff}$$

where  $P_{avg}$  is average power losses,  $P_{cm}$  - power losses in conduction mode,  $P_{bm}$  - internal diode losses,  $P_{son}$  - losses when the MOSFET is switch ON,  $P_{soff}$  - losses when the MOSFET is switch OFF.

Switching losses on power MOSFET can be calculated with the formula:

$$(9) \quad P_{sw} = V_{in} \times I_{out} \times f_{sw} \times \frac{Q_{GS} + Q_{GD}}{I_G}$$

where  $V_{IN} = V_{DS}$  (drain-to-source voltage),  $I_{OUT} = I_D$  (drain current),  $f_{sw}$  is the switching frequency,  $Q_{GS}$  and  $Q_{GD}$  depend on the time the driver takes to charge the FET, and  $I_G$  is the gate current [20].

The temperature rise of the high frequency transformer is given by:

$$(10) \quad \Delta T = \left( \frac{P\Sigma}{A_t} \right)^{0.833}$$

Where  $\Delta T$  = temperature rise in °C,  $P\Sigma$  = total transformer losses (power lost and dissipated as heat) in mW;  $A_T$  = surface area of transformer in  $cm^2$ .

We can express the losses in power switch with:

$$(11) \quad P_q = P_{ON-H} + P_{ON-L} + P_{SW} + P_G + P_D + P_{IC}$$

where  $P_{ON-H}$  and  $P_{ON-L}$  - conductivity losses,  $P_{SW}$  - switching losses,  $P_D$  - dead time losses during switching,  $P_G$  - switching control electrode losses of the switch,  $P_{IC}$  - losses in the driver.

Inductor losses (Steinmetz equation):

$$(12) \quad P_v = C_v f^x B^y$$

$C_v$  - loss coefficient in the ferrite material,  $f$  - losses caused by the influence of frequency and saturation,  $B$  - magnetic flux density [21], [22], [23]. The Watt loss of the ferrite of the inductor at frequency 100kHz are 1500mW/cm<sup>3</sup>. The frequency component  $x$  is 0.722. The calculated inductance of the inductor are  $B = 366mT$ . The turns ratio of the high frequency transformer is 6:1. The Temperature Dependency of Core Loss (Pcv) at 200kHz operating frequency is 1900kW/m<sup>3</sup>. The transformer use a

ferrite core PQ50. The transformer core loss can be calculated by the formula:

$$(13) \quad P_{core} = K_l f^x B^y V_e$$

where  $K_l$  is constant for core material,  $f$  - frequency in kHz,  $B$  - magnetic flux density in kGauss,  $x$  - frequency exponent,  $y$  = flux density exponent,  $V_e$  - effective core volume (cm<sup>3</sup>).

The calculation of the losses in the transformer are made with the methodology used formulas that are frequency dependent. To calculate the switching losses of the transistor were used analytical formulas. The main calculation of the components based of methodology proposed in IEC standard 60205 "Calculation of the effective parameters of magnetic piece parts" [24], [25]

From the results obtained above, the losses in step up and step-down mode are calculated and structured in Table 7.

**Table 7**

*Calculated losses of the isolated converter in step-up and step-down mode*

Losses	Step-up Losses(W)	Step-down Losses(W)
HF Transformer	26.1	25
Inductor	7.9	6.5
Transistor Switching losses	41.5	29.4
Transistor Conduction losses	18.6	11.2
Other	5.2	4.6
Total losses	99.3	76.7

The percentage losses of the converter are shown in Fig.15 (in step-up fig.15a and step-down fig.15b modes). From these two figures, it is calculated that most losses in the converter are caused by the power switches and the transformer. It follows that the cooling system plays an important role in dissipating a significant amount of heat and hence reducing the total losses

### Conclusion

In this article, two mathematical models were created in Simulink and Comsol to analyze the thermal behavior of the power switches and the heat released by each of the main components. An analysis of the main advantages and applications of the considered topology was made.

The model in Matlab allows getting graphically an idea about the change in temperature of the converter at different frequencies and the influence of the heatsink. From the percentage of losses from figures, we can conclude that the losses from the power

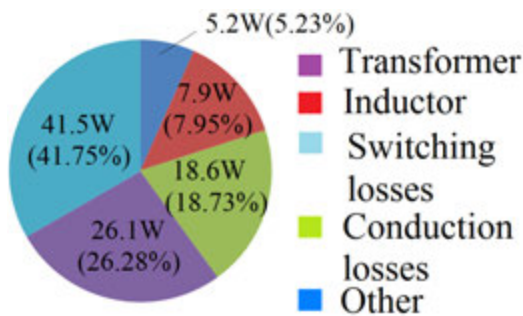


Fig.15.a Percentage losses in Step-up mode.

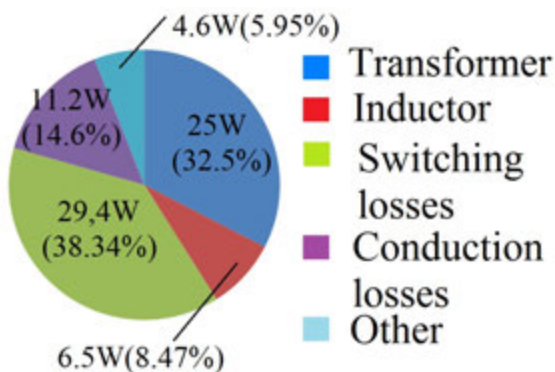


Fig. 15.b Percentage losses in step-down mode.

switches are a major factor in increasing the efficiency of such a converter. In step-down mode are significantly less and close to transformer losses. It is possible that the inductor can be replaced by two inductors on the high and low sides, with Mn-Zn ferrite, which has a significantly higher efficiency at higher frequencies. The influence of the temperature from the power switch through the transition layers to the heatsink is graphically expressed. The three-dimensional model in Comsol graphically shows the amount of heat released by each component of the system. The losses in the main components of the device are considered and, on this basis, the percentage losses in the components are calculated in step-up and step-down mode. For future work, the developed models can serve as a basis for creating more complex models of bidirectional and multilevel DC-DC converters, describing the thermal behavior high frequency transformers and inductors on different level of voltages.

#### Acknowledgement

I would like to express my gratitude for the opportunity to conduct a practical training under the Erasmus Plus program at the University of Ghent, Belgium. Special thanks are due to Prof. Alex Van

den Bossche for his practical tips and advice in this field of science.

#### REFERENCES

- [1] März M., Nance P. Thermal Modeling of Power-electronic Systems// Infineon Technologies AG, Munich, 2000.
- [2] Connor N. What is Heat Equation – Heat Conduction Equation – Definition, 2019, Online Available: <https://www.thermal-engineering.org/what-is-heat-equation-heat-conduction-equation-definition/>
- [3] Vellvehi M., Jorda X., Godignon P., Ferrer C., Milla J. In Coupled electro-thermal simulation of a DC/DC converter // Microelectronics Reliability vol.47, 2007, pp. 2114–2121.
- [4] Asinovski A. Determine MOSFET Junction Temperature and Switching Losses for Various Package Types. Power Management, March 2020.
- [5] Mohamed Ali Belaid1, Ahmed Mohammad Nahhas, Momamed Masmoudi. A Compact Model of Mosfet Transistors Including Dispersion and Thermal Phenomena. Journal of Electrical and Electronic Engineering Vol. 3, Issue 6, December 2015, pp. 192-197.
- [6] Smoot R. How to Select a Heat Sink. <https://www.cuidevices.com/blog/how-to-select-a-heat-sink>
- [7] Guide to Mosfet Power Dissipation Calculation in High-Power Supply, Tutorials 1832, Maxim Integrated Products Inc., 2012, Online Available: <https://www.maximintegrated.com/en/design/technical-documents/tutorials/1/1832.html>
- [8] Thermal expression. <http://hyperphysics.phy-astr.gsu.edu/hbase/thermo/thexp.html>
- [9] Baier J. Accurate Estimation of Losses of Power Inductor in Power Electronics Applications. APEC - Applied Power Electronics Conference and Exposition, 2016.
- [10] 2kW, 48V to 400V, >93% Efficiency, Isolated Bidirectional DC-DC Converter Reference, Design for UPS, TIDA-00951, Texas Instruments <https://www.ti.com/tool/TIDA-00951>
- [11] IXTK120N65X2, IXYS Corporation Datasheet, 2016.
- [12] Reghua. T., V. Mandloi, P. Shrivastava. Compact high voltage, high peak power, high frequency transformer for converter type modulator applications. Published Online: 15 April 2016 Pulsed High Power Microwave Division, Raja Ramanna Centre for Advanced Technology, Indore, M.P. 452013, India.
- [13] Petrović, D., M. Lazić., O. Aleksić, M. Nikolić, V. Ibrahimovic, M. Pajnic. Mn-Zn ferrite line EMI suppressor for power switching noise in the impulse/high current bias regime. Turkish journal of electrical engineering & computer sciences, 26 (5), 2018, pp. 2426-2436.
- [14] Miura Y., M. Kaga, Y. Horita, T. Ise. Bidirectional isolated dual full-bridge dc-dc converter with active clamp

for EDLC. 2010, IEEE Energy Conversion Congress and Exposition, pp. 1136-1143.

[15] Shahab H., A. Moghaddam, A. Ayatollahi, A. Rahmati, Modeling and Current Programmed Control of a Bidirectional Full Bridge DC-DC Converter. Energy and Power Engineering, Vol. 4, No. 3, 2012.

[16] Ramachandran R., M. Nymand, A 98.8% efficient bidirectional full-bridge isolated dc-dc GaN converter. IEEE Applied Power Electronics Conference and Exposition (APEC), 2016, pp. 609-614.

[17] Chitanya K., P. Raghavendran. Isolated Bidirectional Full-Bridge DC-DC Converter with a Flyback Snubber. International Journal of Soft Computing and Engineering (IJSCE), Vol. 3, Issue 2, 2013.

[18] Zhang Y., J. Shi, C. Fu, W. Zhang, P. Wang, J. Li, M. Sumnerk. An Enhanced Hybrid Switching-Frequency Modulation Strategy for Fuel Cell Vehicle Three-Level DC-DC Converters with Quasi-Z Source. Energies. 11. 1026, 2018.

[19] General Thermal Analysis of Integrated Circuits for Power Applications, Technical Articles, 2019, Online Available: <https://www.powerselectronicsnews.com/general-thermal-analysis-of-integrated-circuits-for-power-applications/>

[20] Lakkas G. MOSFET power losses and how they affect power-supply efficiency. Analog Applications Journal, 2016.

[21] Waluyo W., Saodah S., Rohana. Investigation of Transformer Losses and Temperature Rise. Investigation of transformer losses and temperature rise. EEA - Electrotehnica, Electronica, Automatica, Vol. 66, No. 2, 2018, pp. 37-44.

[22] DC/DC Converter. Thermal Management. <https://www.digikey.com/en/pdf/g/gaia-converter/dcdc-converter-thermal-management>.

[23] G. Orenchak G. Estimating Temperature Rise of Transformers. 2004, <https://www.powerselectronics.com/content/article/21861352/estimating-temperature-rise-of-transformers>

[24] Power Losses of an Inductor, Sanwa, <http://www.sanwa-seiden.com/DiynicEditor/ueditor/net/upload/2014-03-19-3818acc4d7-afdf-42da-8ea3-f6721ba91de7.pdf>

[25] Ferrites and accessories: PQ 50/50 Core and accessories, TDK Group, EPCOS AG, 2017, [https://www.tdk-electronics.tdk.com/inf/80/db/fer/pq\\_50\\_50.pdf](https://www.tdk-electronics.tdk.com/inf/80/db/fer/pq_50_50.pdf)

---

*Eng. Evgeni Malev – PhD student in Department of department of "Electronics and microelectronics" in Technical University of Varna*

*Tel.: +359889616620*

*E-mail: [evgeni.malev@tu-varna.bg](mailto:evgeni.malev@tu-varna.bg)*

**Received on: 08.02.2021**

---

## THE FEDERATION OF THE SCIENTIFIC-ENGINEERING UNIONS IN BULGARIA /FNTS/

**is a professional, scientific - educational, nongovernmental, nonpolitical, nonprofit association of legal entities - professional organizations registered under the Law on non-profit legal entities, and their members are engineers, economists and other specialists in the fields of science, technology, economy and agriculture.**

**FNTS has bilateral cooperation treaties with similar organizations in multiple countries.**

**FNTS brings together 19 national associations – Scientific and Technical Unions (STU), 34 territorial associations, which have more than 15 000 professionals across the country.**

**FNTS is a co-founder and member of the World Federation of Engineering Organizations (WFEO).**

**FNTS is a member of the European Federation of National Engineering Associations (FEANI), and a member of the Standing Conference of engineering organizations from Southeast Europe (COPISEE), UN Global Compact, European Young Engineers (EYE). The Federation has the exclusive right to give nominations for the European Engineer (EUR ING) title.**

**Contacts: 108 Rakovsky St., Sofia 1000, Bulgaria**

**WEB: <http://www.fnts.bg>**

**E-mail: [info@fnts.bg](mailto:info@fnts.bg)**